Available online at www.sciencedirect.com
ScienceDirect
Ceramics International 34 (2008) 1023–1026
CERAMICS INTERNATIONAL
www.elsevier.com/locate/ceramint

Low dielectric loss and enhanced tunability of $Ba(Zr_{0.3}Ti_{0.7})O_3$-based thin film by sol–gel method

Lina Gao, Jiwei Zhai *, Xi Yao

Functional Materials Research Laboratory, Tongji University, Shanghai 200092, China

Available online 2 October 2007

Abstract

In this work, dopants and buffer layers were employed to simultaneously lower the dielectric loss and enhance the dielectric tunability of $Ba(Zr_{0.3}Ti_{0.7})O_3$ (BZT) thin films. The BZT, 1 mol% La doping BZT (BZTL) with and without $La_{0.5}Sr_{0.5}CoO_3$ (LSCO) buffer layers were prepared by sol–gel technique. The dielectric properties of the thin films were investigated as a function of frequency and current bias field. As a result, the BZTL thin film with LSCO buffer layer showed lower dielectric loss and higher tunability simultaneously, which can be a promising candidate for tunable microwave device applications.

Keywords: A. Sol–gel processes; C. Dielectric properties; Tunability; BZT thin films

1. Introduction

Barium strontium titanate (BST) thin films have been intensively studied for applications in the high-density dynamic random access memories, monolithic microwave integrated circuit decoupling capacitors, tunable microwave filters, and phased array antennas [1–3]. $Ba(Zr_xTi_{1-x})O_3$ (BZT) is a possible choice as an alternative to BST in the fabrication of ceramic capacitors because Zr^{4+} is chemically more stable than Ti^{4+} and has a larger ionic size to expand the perovskite lattice [4–9]. Therefore, the conduction by electron hopping between Ti^{4+} and Ti^{3+} would be depressed by the substitution of Ti with Zr. The fabrication of BZT thin films by rf-magnetron sputtering [10], sol–gel method [11], and pulsed laser disposition (PLD) [12], and their dielectric properties has been reported recently.

However, many problems remain in utilizing ferroelectric thin films for tunable devices. In particular, one of the major challenges encountered for realizing the integration of ferroelectric thin films into tunable devices is the simultaneous minimization of the materials dielectric loss and maximization of dielectric tunability. Many efforts have been made to improve the dielectric properties of the ferroelectric thin film capacitors, including adding dopants, such as Fe^{2+}, Fe^{3+}, Co^{2+}, Co^{3+}, Mn^{2+}, Mn^{3+}, Ni^{2+}, Mg^{2+}, Al^{2+}, Ga^{3+}, In^{3+}, Cr^{3+}, $Ce^{3+}$and Sc^{3+} [10,13] and using conductive oxide electrodes such as $LaNiO_3$, $La_{0.7}Sr_{0.3}MnO_3$ and yttrium barium copper oxide (YBCO) [14–16]. But few works report the effect of both the dopant and buffer layers on the dielectric properties of BZT thin films. In this work, $Ba(Zr_{0.3}Ti_{0.7})O_3$ (BZT) thin films growth on $Pt/Ti/SiO_2/Si(1\,0\,0)$ substrate, La-doped $Ba(Zr_{0.3}Ti_{0.7})O_3$ (BZTL) thin films growth on $Pt/Ti/SiO_2/Si(1\,0\,0)$ substrate with and without $La_{0.5}Sr_{0.5}CoO_3$ (LSCO) buffer layers were prepared by sol–gel method. The dielectric properties, tunability and figure of merit of the BZT thin films, BZTL thin films with and without LSCO buffer layers were also reported.

2. Experimental procedure

The LSCO buffer layers were prepared from the starting materials: lanthanum acetate $[La(CH_3COO)_3{\cdot}1.5H_2O]$, strontium acetate $[Sr(CH_3COO)_2{\cdot}0.5H_2O]$, and cobalt acetate $[Co(CH_3COO)_2{\cdot}4H_2O]$. The starting materials were mixed with a molar ratio of La:Sr:Co = 1:1:2 and dissolved in heated glacial acetic acid and de-ionized water. An appropriate amount of acetylacetone was added to the solution to stabilize the solution. The concentration of solution was diluted to 0.1 M. For the BZT layer, the calculated amount of barium acetate

* Corresponding author.
E-mail address: apzhai@mail.tongji.edu.cn (J. Zhai).

0272-8842/$34.00
doi:10.1016/j.ceramint.2007.09.076

$[Ba(CH_3COO)_2]$, zirconium(IV) isopropoxide $[Zr(OC_3H_7)_4]$ and titanium(IV) isopropoxide $[Ti(OC_3H_7)_4]$ were used as raw materials to prepare BZT precursor sol. Acetic acid, ethylene glycol monoethyl ether and Acetylacetone were used as solvent and polymerizing agents, respectively. Barium acetate and Lanthanum acetate (concentration range: 0 and 1 mol%) were heated and dissolved in acetic acid. After cooling to room temperature, $Zr(OC_3H_7)_4$ and $Ti(OC_3H_7)_4$ were added in this solution. The ethylene glycol monoethyl ether and acetylacetone were added to control the viscosity and cracking of films and the solution was mixed and refluxed for 1 h. The concentration of the final solution was adjusted to 0.3 M.

The LSCO buffer layers were prepared by spin coating on the Pt/Ti/SiO_2/Si(1 0 0) substrates at 3000 rpm for 20 s each layer. Each spin-coated LSCO layer was subsequently heat-treated in air at 500 °C on a hot plate for 10 min. The coating and heat treatment procedures were repeated until reaching the desired thickness. Finally, the samples were heated at 700 °C for 30 min to crystalline the LSCO amorphous films.

The BZT layers were deposited on the Pt/Ti/SiO_2/Si(1 0 0), BZTL layers were deposited on the Pt/Ti/SiO_2/Si(1 0 0) and LSCO buffered Pt/Ti/SiO_2/Si(1 0 0) substrates, respectively, using the same coating process. Finally, LSCO films with a thickness of 30 nm, BZT and BZTL films with a thickness of 450 nm were grown in this study.

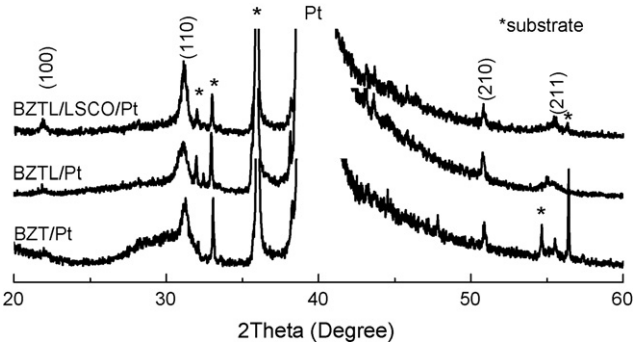

Fig. 1. XRD patterns of BZT/Pt, BZTL/Pt and BZTL/LSCO/Pt thin films.

The crystalline phase of the thin films was identified by X-ray diffraction (BRUKER D8 Advance diffract meter). The surface morphology of the films was studied using field-emission scanning electron microscopy (FEI Quanta 200 FEG). For the electrical measurements the top gold electrode 500 μm square was deposited by DC-sputtering. The current–voltage

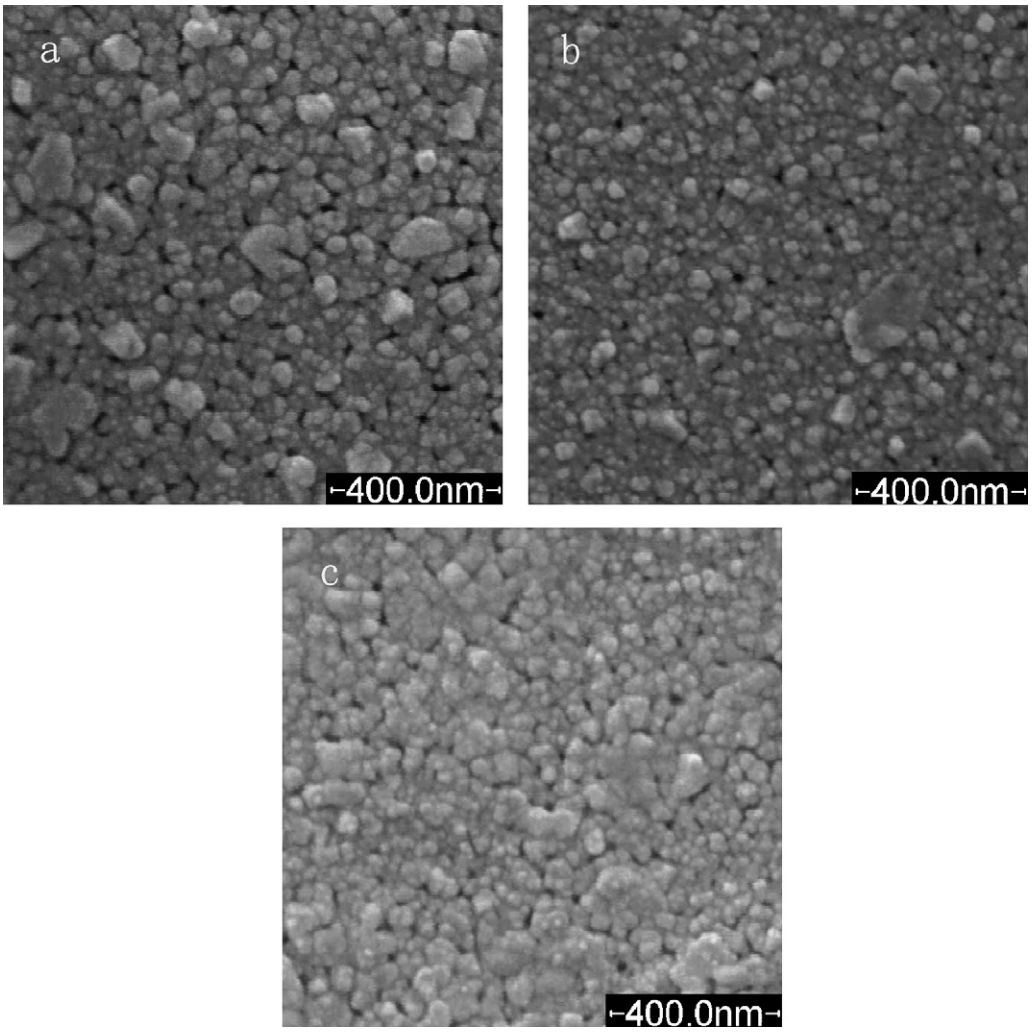

Fig. 2. FE-SEM images of BZT/Pt, BZTL/Pt and BZTL/LSCO/Pt thin films: (a) BZT/Pt, (b) BZTL/Pt, and (c) BZTL/LSCO/Pt.

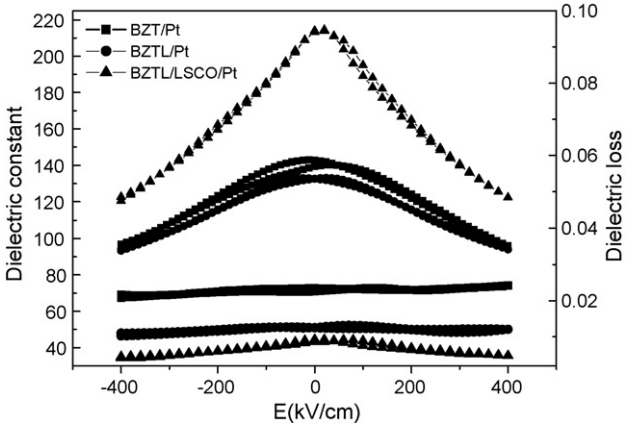

Fig. 3. Dielectric constant and dielectric loss of BZT/Pt, BZTL/Pt and BZTL/LSCO/Pt thin films with applied dc field at 1 MHz.

(*I–V*) characteristics were measured using a Keithley 6517A. The capacitance–voltage (*C–V*) was measured using an HP4284A impedance analyzer.

3. Results and discussion

The X-ray diffraction patterns of the BZT thin film, BZTL thin films with and without LSCO buffer layers annealed at 700 °C were shown in Fig. 1. The X-ray patterns indicated that the samples were perovskite and polycrystalline structure and can be characterized by the appearance of (1 0 0), (1 1 0), (2 0 0), (2 1 0) and (2 1 1) peaks in the XRD spectra. The polycrystalline nature in these thin films was due to a lattice mismatch between BZT thin film and the Pt/Ti/SiO_2/Si(1 0 0) substrates [17]. In comparison with the BZTL film without buffer layers, the full-width-at-maximum (FWHM) of BZTL film with LSCO buffer layers decreased indicating an increase in grain size.

The surface morphological features of BZT thin film, BZTL thin films with and without LSCO buffer layers were determined by field-emission scanning electron microscope (FE-SEM). Fig. 2 shows the FE-SEM images of surface of the BZT thin film, BZTL thin films on the Pt/Ti/SiO_2/Si(1 0 0) substrates with and without LSCO buffer layers. It was found that surface morphologies of the films were morphologically smooth and crack free. As shown in Fig. 2, the surface morphological features of the films appeared to be quite sensitive to the concentration of La dopant and LSCO buffer layers. Comparing the BZT thin film, the BZTL thin film showed smaller grain size. However, the BZTL thin film with LSCO buffer layers showed bigger average grain size than those without LSCO buffer layers. This result suggested that the LSCO buffer layers substantially influence the crystallization behavior and the microstructure of BZTL thin films. This FE-SEM results were in excellent agreement with the X-ray diffraction data.

The dielectric properties of the BZT thin films in an Au/BZT/Pt configuration were measured at room temperature as a function of the applied frequency and dc electric field. Fig. 3 shows the dielectric constant and the dielectric loss of the BZT thin film, BZTL thin films with and without LSCO buffer layers at a frequency of 1000 kHz. The dielectric constant and dielectric loss were decreased with increasing applied dc field. The change of dielectric constant with dc electric field at the paraelectric phase of the material results from anharmonic interaction of titanium ions in perovskite structure [18].

Table 1 summarized the dielectric properties, tunability, figure of merit and leakage current of the BZT thin films, BZTL thin films with and without LSCO buffer layers measured at a frequency of 1000 kHz. The tunability is defined as $(\varepsilon_{max} - \varepsilon_{min})/\varepsilon_{max}$, where ε_{max} and ε_{min} are maximum and minimum values of dielectric constant, respectively, measured at the zero electric field and 400 kV/cm electric field, respectively. The figure of merit (FOM) is a parameter to characterize correlations between tunability and dielectric loss. This parameter is defined as FOM = [tunability (%)/tan δ (%)], where dielectric loss is given on a percentage scale. The figure of merit reflects the fact that a tunable microwave circuit cannot take full advantage of high tunability if the loss factor is high [19]. As compared with the BZT thin film, the BZTL film without LSCO buffer layers showed lower dielectric constant, dielectric loss, tenability (at 400 kV/cm) and leakage current (at 400 kV/cm). Generally, when La^{3+}, Bi^{3+}, Ce^{3+} ions (act as ''A'' site donor dopants in ABO_3 perovskite lattice) substitute Ba^{2+}, the inherent oxygen vacancies concentration are suppressed when formed at the top electrode/BZT interface [20]. While the BZTL film with LSCO buffer layers showed higher dielectric constant, tunability and figure of merit showed lower dielectric loss than the other thin films. Generally, interfaces between the ferroelectric thin films and the electrodes affect the measured dielectric properties. It has been proposed that the reduction of ε_r in ferroelectric thin films can be explained by the existence of interfacial ''dead layer'' at one or both metal electrodes with poor dielectric properties [21]. They may arise from the oxygen interdiffusion, chemical reaction, structural defects, or Schottky barriers at the interfaces. Use of conductive oxide electrodes, such as (La, Sr) MnO_3, $LaNiO_3$, and YBCO, can decrease the thickness of the dead layer and enhance the dielectric constant and tenability [22,23]. In addition, the decreased dielectric loss of BZTL thin films with LSCO buffer

Table 1
Dielectric properties of BZT/Pt, BZTL/Pt and BZTL/LSCO/Pt thin films at 1 MHz and at room temperature

	Dielectric constant	Dielectric loss	Tunability (%) (400 kV/cm)	FOM	Leakage current (A/cm^2) (400 kV/cm)
BZT	139.3	0.022	30.9	13.7	1.39×10^{-4}
BZTL/Pt	132.6	0.012	29.5	23.6	1.94×10^{-5}
BZTL/LSCO/Pt	213.1	0.009	42.7	47.4	5.43×10^{-5}

layers may be due to the excellent film quality and the absence of interfacial barriers of the BZTL/LSCO heterostructure.

4. Conclusions

In this study, BZT and BZTL thin films with and without LSCO buffer layer were successfully fabricated by sol–gel technique on Pt/Ti/SiO_2/Si(1 0 0) substrates. The XRD patterns revealed that all the films were polycrystalline and single perovskite phase. The FE-SEM image showed that the average grain size of the BZTL film with LSCO buffer layer was larger than that of the BZTL film without buffer layer. The BZTL film with LSCO buffer layer showed enhanced properties with low dielectric loss, low leakage current, high tunability and FOM value as compared to the BZT thin film. The improved dielectric properties such as dielectric loss, tunability and FOM of BZTL thin films with LSCO buffer layer suggested their suitability for tunable microwave applications.

Acknowledgements

This work was supported by the Ministry of Sciences and Technology of China through 973-Project under grant 2002CB613304, Shanghai Nano Fundamental Committee under contract No. 05nm05028, Program for New Century Excellent Talents in University and Specialized Research Fund for the Doctoral Program of Higher Education (SRFDP20060247003).

References

[1] D.E. Kotecki, A review of high dielectric materials for DRAM capacitors, Integr. Ferroelectr. 16 (1997) 1–19.
[2] F. De Flaviis, O.M. Stafsudd, N.G. Alexopoulos, Planar microwave integrated phase shifter design with high purity ferroelectric materials, IEEE Trans. Microw. Theory Tech. 45 (1997) 963–969.
[3] R. Babbitt, T. Koscica, W. Drach, L. Didomenico, Ferroelectric phase shifters and their performance in microwave phased array antennas, Integr. Ferroelectr. 8 (1995) 65–76.
[4] P.W. Rehrig, S.E. Park, S. Trolier-MsKinstry, G.L. Messing, B. Jones, T.R. Shrout, Piezoelectric properties of zirconium-doped barium titanate single crystals grown by templated grain growth, J. Appl. Phys. 86 (1999) 1657–1661.
[5] J. Zhai, C. Haydn, Nonlinear behaviors of the compositionally graded (Ba,Sr)TiO_3 thin films derived by a sol–gel process, Appl. Phys. Lett. 84 (2004) 1162–1164.
[6] Y. Zhi, A. Chen, R. Guo, A.S. Bhalla, Ferroelectric-relaxor behavior of $Ba(Ti_{0.7}Zr_{0.3})O_3$ ceramics, J. Appl. Phys. 92 (2002) 2655–2657.
[7] S.M. Mukhopadhyay, T.C.S. Chen, Surface chemical states of barium titanate: influence of sample processing, J. Mater. Res. 10 (1995), 1502–1057.
[8] S. Hoffmann, R. Waser, Control of the morphology of CSD-prepared (Ba,Sr)TiO_3 thin films, J. Eur. Ceram. Soc. 19 (1999) 1339–1343.
[9] A. Dixit, S.B. Majumder, A. Savvinov, R.S. Katiyar, R. Guo, A.S. Bhalla, Investigations on the sol–gel-derived barium zirconium titanate thin films, Mater. Lett. 56 (2002) 933–940.
[10] W.S. Choi, J. Yi, B. Hong, The effect of cerium doping in barium zirconate titanate thin films deposited by rf-magnetron sputtering system, Mater. Sci. Eng. B 109 (2004) 146–151.
[11] A. Dixit, S.B. Majumder, R.S. Katiyar, A.S. Bhalla, Relaxor behavior in sol–gel-derived $BaZr_{(0.40)}Ti_{(0.60)}O_3$ thin films, Appl. Phys. Lett. 82 (2003) 2679–2681.
[12] R. James, C. Prakash, Ferroelectric properties of pulsed laser deposited $Ba(Zr_{0.15}Ti_{0.85})O_3$ thin films, Appl. Phys. Lett. 84 (2004) 1165–1167.
[13] M.W. Cole, P.C. Joshi, M.H. Ervin, M.C. Wood, R.L. Pfeffer, The influence of Mg doping on the materials properties of $Ba_{1-x}Sr_xTiO_3$ thin films for tunable device applications, Thin solid Films 374 (2000) 34–41.
[14] K.H. Yoon, J.H. Sohn, B.D. Lee, Effect of $LaNiO_3$ interlayer on dielectric properties of $(Ba_{0.5}Sr_{0.5})TiO_3$ thin films deposited on differently oriented Pt electrodes, Appl. Phys. Lett. 81 (2002) 5012–5014.
[15] S.G. Lu, X.H. Zhu, C.L. Mak, K.H. Wong, H.L.W. Chan, C.L. Choy, High tunability in compositionally graded epitaxial barium strontium titanate thin films by pulsed-laser deposition, Appl. Phys. Lett. 82 (2003) 2877–2879.
[16] D. Galt, J.C. Price, J.A. Beall, R.H. Ono, Characterization of a tunable thin film microwave $YBa_2Cu_3O_{7-x}$/$SrTiO_3$ coplanar capacitor, Appl. Phys. Lett. 63 (1993) 3078–3080.
[17] S.T. Lee, N. Fujimura, T. Ito, Epitaxial growth of $BaTiO_3$ thin films and their internal stresses, Jpn. J. Appl. Phys. 34 (1995) 5168–5171.
[18] L. Wu, Y.-C. Chen, Y.-P. Chou, Y.-Y. Tsai, S.-Y. Chu, Dielectric properties of Al_2O_3-doped barium strontium titanate for application in phased array antennas, Jpn. J. Appl. Phys. 38 (1999) 5154–5161.
[19] D. Dimos, M.V. Raymond, R.W. Schwartz, H.W. Al-Shareef, C.H. Mueller, Tunability and calculation of the dielectric constant of capacitor structures with interdigital electrodes, J. Electroceram. 2 (1997) 145–153.
[20] K.T. Kim, C.I. Kim, Structure and dielectric properties of Bi-doped $Ba_{0.6}Sr_{0.4}TiO_3$ thin films fabricated by sol–gel method, Microelectric Eng. 66 (2003) 835–841.
[21] X.X. Xi, H.C. Li, W.D. Si, A.A. Sirenko, I.A. Akimov, J.R. Fox, A.M. Clark, J.H. Hao, Oxide thin films for tunable microwave devices, J. Electroceram. 4 (2000) 393–405.
[22] X.G. Tang, H.Y. Tian, J. Wang, K.H. Wong, H.L.W. Chan, Effect of $CaRuO_3$ interlayer on the dielectric properties of Ba(Zr,Ti)O_3 thin films prepared by pulsed laser deposition, Appl. Phys. Lett. 89 (2006) (142911-1-3).
[23] H. Chen, J. Yang, L. Miao, L.X. Zhao, B. Cao, X.G. Xu, B.R. Qiu, Zhao, Leakage current of Pt/$(Ba_{0.7}Sr_{0.3})TiO_3$ interface with dead layer, J. Appl. Phys. 97 (2005) (024106-1-4).